



Available online at www.sciencedirect.com

SCIENCE @ DIRECT®

C. R. Mecanique 333 (2005) 688–693



MECANIQUE

<http://france.elsevier.com/direct/CRAS2B/>

Computational AeroAcoustics: from acoustic sources modeling to farfield radiated noise prediction
Acoustic source terms study for non-isothermal flows using an aeroacoustic hybrid approach

François Golanski *, Christian Prax

Laboratoire d'études aérodynamiques, université de Poitiers, UMR CNRS 6609, bâtiment K, 40, avenue du recteur Pineau, 86000 Poitiers, France

Available online 8 September 2005

Abstract

This paper presents a numerical study of noise source term in non-isothermal flows in the context of an aeroacoustic hybrid technique at low Mach numbers. Asymptotic analysis applied to the fully compressible Navier–Stokes equations provides separated sets of equations for the dynamic of the flow and the production and propagation of acoustic waves. Comparisons with analytical dipole and quadrupole distributions are performed, confirming the dipole type of non-isothermal source distribution. This paper is a preliminary work for some more extensive studies on the topic. *To cite this article: F. Golanski, C. Prax, C. R. Mecanique 333 (2005).*

© 2005 Académie des sciences. Published by Elsevier SAS. All rights reserved.

Résumé

Étude des sources acoustiques pour des écoulements anisothermes par une méthode aéroacoustique hybride. Cet article présente une étude numérique des sources acoustiques dans le cas d'écoulements anisothermes à faibles nombres de Mach. Un développement asymptotique des équations de Navier–Stokes compressibles fournit des systèmes d'équations séparés pour la dynamique de l'écoulement et pour la génération et la propagation acoustique. Des comparaisons à des distributions de sources analytiques de types dipolaire et quadripolaire confirment la nature dipolaire de la composante des sources liée aux fluctuations de température. *Pour citer cet article : F. Golanski, C. Prax, C. R. Mecanique 333 (2005).*

© 2005 Académie des sciences. Published by Elsevier SAS. All rights reserved.

Keywords: Acoustics; Aeroacoustic sources; Non-isothermal flow; Low Mach number

Mots-clés : Acoustique ; Sources aéroacoustiques ; Écoulements anisothermes ; Faibles nombres de Mach

* Corresponding author.

E-mail addresses: francois.golanski@lea.univ-poitiers.fr (F. Golanski), christian.prax@lea.univ-poitiers.fr (C. Prax).

1. Introduction

In the case of free low Mach number flows, the computational time of compressible DNS (Direct Numerical Simulation) is dramatically increased by the presence of acoustics, whereas it does not act on dynamics phenomenon. Then, a hybrid approach composed of incompressible models coupled to an aeroacoustic analogy makes possible to reduce the computational cost. For non-isothermal flows, a quasi-incompressible model allows one to neglect the density variations due to compressibility effects (such as acoustic waves) while density variations due to temperature inhomogeneities are kept. The formulation is briefly described in the first part. The second part explains how appropriate acoustic source terms for LEE (Linearized Euler’s Equations) computation are derived from the corresponding dynamic simulation. In the context of physical analysis, this type of approach exhibits the advantage of making possible the splitting of the different terms of the equations, so the last part explores the comparison of different acoustic source terms contributions.

2. The low Mach number flow approximation

The CFD part of the aeroacoustic hybrid approach presented in this paper is performed using a low Mach number approximation (called LMNA throughout this document). In what follows, all quantities are used in non-dimensional form and the superscript * indicates dimensional ones. The reference quantities are L_{ref}^* , U_{ref}^* , T_{ref}^* , ρ_{ref}^* for lengths, velocities, temperatures and densities. The time reference is $t_{ref}^* = L_{ref}^*/U_{ref}^*$. The three fundamental non-dimensional parameters are the Reynolds number $Re = \rho_{ref}^* U_{ref}^* L_{ref}^* / \mu_{ref}^*$, the Prandtl number $Pr = \mu_{ref}^* c_p^* / k^*$ and the Mach number defined as $M = U_{ref}^* / \sqrt{\gamma r^* T_{ref}^*}$. Starting from the fully compressible Navier–Stokes equations for a perfect gas, the LMNA is obtained [1,2] by expanding all variables of the flow (ρ , u_i , p , T) in power series of the small parameter $\epsilon = \gamma M^2$. The development is the same for ρ , u_i and T : $\rho = \rho^{(0)} + \epsilon \rho^{(1)}$. For the pressure, the perfect gas law imposes the decomposition $p = \frac{p^{(0)}}{\epsilon} + p^{(1)}$. At the lowest order, the following system is obtained:

$$\frac{\partial \rho^{(0)}}{\partial t} + \frac{\partial \rho^{(0)} u_i^{(0)}}{\partial x_i} = 0 \tag{1}$$

$$\frac{\partial p^{(0)}}{\partial x_i} = 0 \quad (\forall i = 1, 2, 3) \tag{2}$$

$$\rho^{(0)} \frac{\partial u_i^{(0)}}{\partial x_i} = \frac{1}{Re Pr T^{(0)}} \frac{\partial^2 T^{(0)}}{\partial x_i^2} \tag{3}$$

$$p^{(0)} = \rho^{(0)} T^{(0)} \tag{4}$$

Eq. (2) indicates clearly that the pressure term $p^{(0)}$ is spatially uniform. In the present case which concerns only open physical domains, this term is also constant in time. The system of Eqs. (1)–(4) is closed by the momentum conservation equation, expanded to the zeroth-order in ϵ

$$\frac{\partial \rho^{(0)} u_i^{(0)}}{\partial t} + \frac{\partial \rho^{(0)} u_i^{(0)} u_j^{(0)}}{\partial x_j} = - \frac{\partial p^{(1)}}{\partial x_i} + \frac{1}{Re} \frac{\partial \tau_{ij}^{(0)}}{\partial x_j} \tag{5}$$

Finally, the LMNA system is composed of Eqs. (1)–(5).

In the hybrid approach context, the LMNA has the interesting properties of not containing acoustic waves [1], while temperature inhomogeneities effects on dynamics are kept.

3. Restoring acoustic motion from a LMNA simulation

Starting from the CFD model for non-isothermal low Mach number flows, acoustic motion can be restored in a second step. In the case of isothermal flows, the acoustic source terms are now well known [3], and it has been shown that non-isothermal cases require supplementary source terms.

The ε expansion of the compressible Navier–Stokes equations is continued with the higher order and suitable assumptions are used to derive the LEE which in turns give the source terms (this development is detailed in [4]). The LEE for a perturbation $(\rho^{(1)}, u_i^{(1)}, p^{(1)})$ over a steady mean flow $(\rho^{(0)}, u_i^{(0)}, p^{(0)}, T^{(0)})$ are thus obtained:

$$\frac{\partial \rho^{(1)}}{\partial t} + \frac{\partial}{\partial x_j} (\rho^{(0)} u_j^{(1)} + \rho^{(1)} u_j^{(0)}) = 0 \tag{6}$$

$$\frac{\partial \rho^{(0)} u_i^{(1)}}{\partial t} + (\rho^{(0)} u_j^{(1)} + \rho^{(1)} u_j^{(0)}) \frac{\partial u_j^{(0)}}{\partial x_j} + \frac{\partial \rho^{(0)} u_i^{(0)} u_j^{(1)}}{\partial x_j} + \frac{\partial p^{(1)}}{\partial x_i} = S_i \tag{7}$$

$$\frac{\partial p^{(1)}}{\partial t} + \frac{\partial}{\partial x_j} (\rho^{(0)} u_j^{(1)} + \gamma p^{(1)} u_j^{(0)}) + (\gamma - 1) p^{(1)} \frac{\partial u_j^{(0)}}{\partial x_j} = 0 \tag{8}$$

where S_i stands for the acoustic sources, with

$$S_i = \underbrace{-\frac{\partial \rho^{(0)} u_i^{(0)}}{\partial t}}_{S_i^t} - \underbrace{\frac{\partial \rho^{(0)} u_i^{(0)} u_j^{(0)}}{\partial x_j}}_{S_i^x} \tag{9}$$

This expression is consistent with the one defined in [3] where the term $\frac{\partial \rho^{(0)} u_i^{(0)}}{\partial t}$ is absent: this term is divergence free in isothermal configurations and in consequence does not excite the acoustic mode. This is no more the case with non-isothermal flows and it generates a part of the radiated noise. This term involves temporal fluctuations of momentum in the case where the density distribution is not homogeneous.

4. Test case: non-isothermal temporal mixing layer

The temporally evolving mixing layer, chosen to study the separated contributions of the different parts of the source terms, occurs in a rectangular domain between two streams of different characteristics (Fig. 1). This flow configuration has already been used for the validation of the non-isothermal source terms. It presents the advantage of reducing the computational costs of simulations and the periodicity in the streamwise direction makes

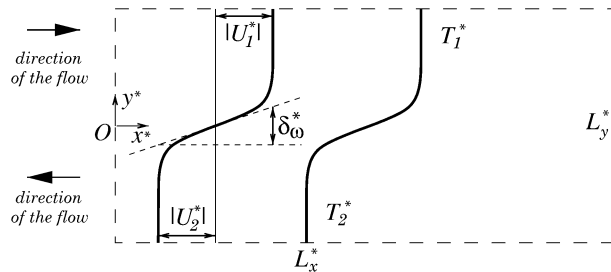


Fig. 1. The temporal mixing layer flow configuration.

Fig. 1. La configuration de couche de mélange temporelle.

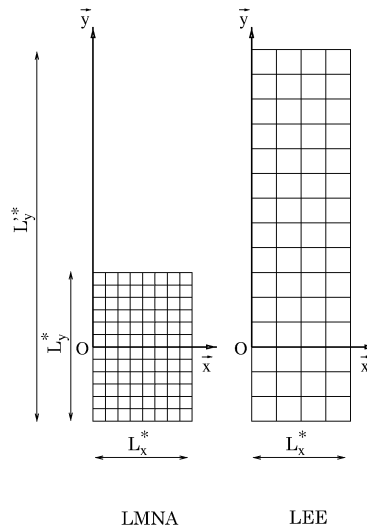


Fig. 2. Representation of the different computational grids.

Fig. 2. Représentation des différents maillages.

it possible to avoid the sensitive question of the outflow boundary condition. The flow and acoustic computations are performed on Cartesian grids. The spatial derivatives are computed by sixth-order compact finite difference scheme of [5]. The temporal integrations are realised by using a third order Runge–Kutta scheme in the LMNA resolution and a fourth-order one in the LEE resolution. The temporal derivation of the source term (9) is performed by a third-order explicit approximation. The boundary conditions of the LMNA simulation are periodic in the streamwise direction, and free-slip in the y -direction. In the LEE case, a periodic condition is also used in the x -direction, whereas the NRBC of [6] is used in the other one. The LEE simulation is performed on a coarser grid than the LMNA one. The source terms are computed on the LMNA grid and only one point out of two is kept to solve the LEE. Fig. 2 shows the different computational grids used in this paper. The references are chosen to be $L_{\text{ref}}^* = \delta_\omega^*$, $U_{\text{ref}}^* = U_1^* - U_2^*$ and $\rho_{\text{ref}}^* = \rho_2^*$. The Reynolds number of the flow is $Re = 400$, and the aeroacoustic simulation is dimensioned to correspond to a Mach number $M = 0.2$ flow. The initial mean velocity field is a hyperbolic tangent profile. Three modes of perturbation are superimposed to destabilise the flow. The three modes are the most unstable one of the hyperbolic tangent profile (with a wavelength λ_p) and the first two subharmonic. Then, the mixing layer develops by the creation of four initial vortices followed by two successive pairings. The LMNA simulation extends from $y = -30$ to $y = 30$. In the LEE simulation, the physical domain is extended at the top to $y = 120$ in order to observe the acoustic fields in a region of space where the forcing terms are equal to zero. In order to observe the four initial vortices, L_x is fixed to $L_x = 4\lambda_p$. The computational grids contain respectively 256×501 and 128×626 points for the LMNA and the LEE simulations.

5. Source terms contributions

Lighthill’s analogy was used in some other studies on the non-isothermal mixing layer [7,8]. Analysis of numerical results on the amplitude of ‘plane waves’ were performed by considering the mean part of the density perturbations $\langle \rho^{(1)} \rangle$ (defined as $\langle \rho^{(1)} \rangle(y, t) = \frac{1}{L_x} \int_0^{L_x} \rho^{(1)}(x, y, t) dx$) arriving at the boundary of the numerical domain. It appears that each part of the source contributes notably to the radiated noise. The topology of the fields radiated by the separated sources is now accessible in the hybrid approach. Simulations presented here were per-

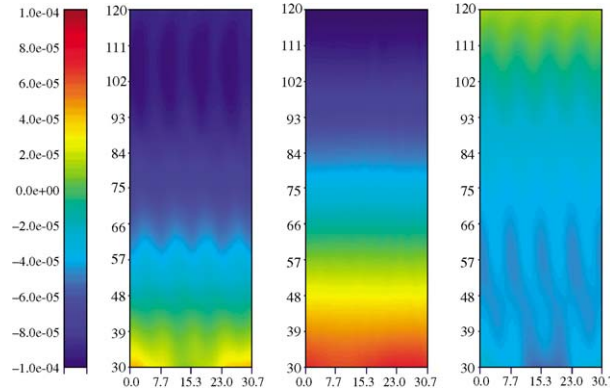


Fig. 3. Density field $\rho^{(1)}$ in the acoustic propagation zone at $t = 170$. Left: Full source term; Middle: S_i^t only; Right: S_i^x only.

Fig. 3. Champ de masse volumique $\rho^{(1)}$ dans la région de propagation à $t = 170$. Gauche : Source terme complet ; milieu : S_i^t seul ; droite : S_i^x seul.

formed (with $M = 0.2$ and an initial temperature ratio of 2) for the full source term and for the separate terms S_i^t and S_i^x .

Before any comment on the radiated fields, some precisions are useful to understand the representation of acoustic propagation resulting from the temporal model. The periodicity condition in the x -direction remains equivalent to consider an infinite distribution of sources emitting at the same time with the same characteristics: when wave trains are emitted with an x -direction component, waves from mirror sources can travel through periodic boundaries and create interferences in the observation domain. This effect is particularly true if waves are emitted in a near horizontal direction. On the other hand, if they are emitted mainly in the y -direction, waves fronts are observed as horizontal fronts propagating to the top (or the bottom) without interference patterns. Whatever, Fig. 3 shows clearly that S_i^t and S_i^x contributions present different types of emissions. Horizontal fronts for S_i^t let us suppose an emission mainly oriented in the direction normal to the mean flow while interferences are present in the S_i^x emission and reveal a different directivity. In the literature on isothermal flows, S_i^x is known to contribute as a quadrupole distribution and according to [9], the temperature fluctuations involve dipole terms in radiated fields. In order to check this point, a simplified model of dipole and quadrupole sources is implemented to visualize the corresponding radiated fields.

Fig. 4 shows density fields radiated by four analytic quadrupole and dipole sources all centered at $y_c = 0$ and respectively defined as: $S_i = \frac{\partial T_{ij}}{\partial x_j}$ where

$$T_{ij} = A \frac{L_x}{4\pi} \begin{bmatrix} -\cos[4\pi(x - x_c)/L_x] e^{-\alpha(y-y_c)^2} & 0 \\ 0 & \cos[4\pi(y - y_c)/L_x] e^{-\alpha(x-x_c)^2} \end{bmatrix} \sin(\omega t) \tag{10}$$

and $S_i = F_i$ with

$$\begin{cases} F_1 = 0 \\ F_2 = A \cos[4\pi(y - y_c)/L_x] e^{-\alpha(x-x_c)^2} \sin(\omega t) \end{cases} \tag{11}$$

The parameters of these sources are $A = 0.01$, $\alpha = \ln(2)/5$ and $\omega = 2\pi c_2/(2L_x)$. The time step of the simulation is $dt = 0.15$. The dipole sources are defined on $(x, y) \in [0, L_x] \times [y_c - L_x/8, y_c + L_x/8]$, and the quadrupole sources on $(x, y) \in [x_c - L_x/8, x_c + L_x/8] \times [y_c - L_x/8, y_c + L_x/8]$.

The fields generated by analytical sources present some similarities with those obtained with separate contributions of noise emitted by the flow. The interference patterns present in S_i^x emission are comparable to those observed in quadrupolar emission. Horizontal waves let us assume the suspected dipolar nature of S_i^t .

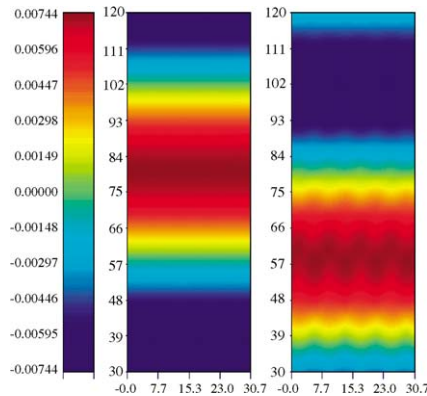


Fig. 4. Density fields $\rho^{(1)}$ radiated by analytical distributions of four dipolar sources (on the left) and four quadrupolar sources (on the right).

Fig. 4. Champ de masse volumique $\rho^{(1)}$ rayonné par une distribution analytique de quatre sources dipolaires (à gauche) et quatre sources quadripolaires (à droite).

6. Conclusion

Numerical investigation of noise radiated by a non-isothermal mixing layer in temporal evolution has been performed using an aeroacoustic hybrid method for low Mach number flows. Comparison of separate acoustic density fields produced by different parts of source terms was realised. Differences between the directivity patterns have been detected despite the particular acoustic propagation characteristics related to the temporal model. Similar fields have been observed by modeling dipoles and quadrupoles analytical source distributions confirming that temperature fluctuations induce dipole type sources. However, this preliminary study shows the potential of this type of approach for the analysis of sound sources in inhomogeneous flows.

Acknowledgements

We are grateful to Professor Eric Lamballais for his invaluable assistance. Computations were carried out at the IDRIS (Institut du développement et des ressources en informatique scientifique, Paris).

References

- [1] P.A. McMurtry, W.-H. Jou, J.J. Riley, R.W. Metcalfe, Direct numerical simulations of a reacting mixing layer with chemical heat release, *AIAA J.* 24 (6) (1986) 962–970.
- [2] A. Cook, J. Riley, Direct numerical simulation of a turbulent reactive plume on a parallel computer, *J. Comput. Phys.* 129 (1996) 263–283.
- [3] C. Bogey, C. Bailly, D. Juvé, Computation of flow noise using source terms in linearized Euler's equations, *AIAA J.* 40 (2) (2002) 235–243.
- [4] F. Golanski, C. Prax, E. Lamballais, V. Fortuné, J.-C. Valière, An aeroacoustic hybrid approach for non-isothermal flows at low Mach number, *Int. J. Numer. Methods Fluids* 45 (2004) 441–461.
- [5] S.K. Lele, Compact finite difference scheme with spectral-like resolution, *J. Comput. Phys.* 103 (1992) 16–42.
- [6] M.B. Giles, Nonreflecting boundary conditions for Euler equation calculations, *AIAA J.* 28 (12) (1989) 2050–2058.
- [7] V. Fortuné, E. Lamballais, Y. Gervais, Etude par simulation numérique directe temporelle des effets de la température sur l'émission acoustique des couches de mélange, *C. R. Acad. Sci.* 328 (2000) 693–700.
- [8] F. Golanski, V. Fortuné, E. Lamballais, Prediction of noise radiated by a non-isothermal mixing layer using a low Mach number approximation, in: *RTO AVT Symposium on Aging Mechanisms and Control: Part A – Developments in Computational Aero- and Hydro-Acoustics*, Manchester, UK, RTO-MP-079(I), 2001.
- [9] G.M. Lilley, Jet noise classical theory and experiments, in: H.H. Hubbard (Ed.), *Aeroacoustics of Flight Vehicles: Theory and Practice*, vol. 1: Noise Sources, NASA technical report 90-3052, 1991, pp. 211–289.